processes

MDPI

Article

Heat-Sealing Process for Chañar Brea Gum Films

María Fernanda Torres [1,*], Federico Becerra [1], Mauricio Filippa [2], Gisela Melo [3] and Martin Masuelli [1,*]

[1] Instituto de Física Aplicada (INFAP-CONICET-UNSL), Departamento de Química, Facultad de Química, Bioquímica y Farmacia, Universidad Nacional de San Luis, Ejército de los Andes 950, San Luis 5700, ZC, Argentina; federicobecerra456@gmail.com
[2] Departamento de Farmacia, Facultad de Química, Bioquímica y Farmacia, Universidad Nacional de San Luis, Ejército de los Andes 950, San Luis 5700, ZC, Argentina; mauricio.filippa@gmail.com
[3] Facultad de Química, Bioquímica y Farmacia, IMIBIO-CONICET, Universidad Nacional de San Luis, Chacabuco 917, San Luis 5700, ZC, Argentina; gisela22arg@gmail.com
* Correspondence: fpeder21@gmail.com (M.F.T.); masuelli@unsl.edu.ar or masuellimartin94@gmail.com (M.M.)

Abstract

This work presents a comprehensive evaluation of the heat-sealability of films developed from chañar brea gum (CBG), a biopolymer with potential for packaging applications. Heat sealability is a critical property in the packaging industry, as it directly determines the integrity and functionality of the final product. The films were prepared by the 10% casting method with the addition of glycerin, and heat sealing was performed at 140 °C using a heat sealer. Heat sealing was performed on 2 cm × 10 cm strips of chañar brea gum in the horizontal (CBG-H) and vertical (CBG-V) directions. This study employs a joint determination to explore the fundamental properties of the films, including proximate analysis, antioxidant capacity, FTIR, DSC, TGA-DTGA, XRD, mechanical testing, water vapor permeability, sorption, and biodegradability. By integrating the results of all these determinations, this study seeks to evaluate and explain the "intimate relationships"—i.e., the complex interconnections among the molecular structure, composition, thermal behavior, mechanical properties, and barrier properties of chañar brea gum films—and how these fundamental properties dictate and control their heat sealability. The thermal stability of CBG is up to 200 °C, with a melting point of 152.48 °C. The interstrand spacing was very similar at 4.88 nm for CBG and 4.66 nm for CBG-H. The SEM images of the heat seal show rounded shapes on the surface, while in the cross section, it is homogeneous and almost without gaps. The WVP decreased from 1.7 to 0.37 for CBG and CBG-H, respectively. The Young's modulus decreased from 132 MPa for CBG to 96.5 MPa for CBG-H. The heat sealability is 656 N/m, with a biodegradability of 4 days. This comprehensive approach is crucial for optimizing the sealing process and designing functional and efficient biodegradable packages.

Keywords: chañar brea gum; heat-sealed; films

check for updates

Academic Editor: Sara Liparoti

Received: 26 May 2025
Revised: 23 June 2025
Accepted: 3 July 2025
Published: 9 July 2025

Citation: Torres, M.F.; Becerra, F.; Filippa, M.; Melo, G.; Masuelli, M. Heat-Sealing Process for Chañar Brea Gum Films. *Processes* **2025**, *13*, 2189. https://doi.org/10.3390/pr13072189

Correction Statement: This article has been republished with a minor change. The change does not affect the scientific content of the article and further details are available within the backmatter of the website version of this article.

Copyright: © 2025 by the authors. Licensee MDPI, Basel, Switzerland. This article is an open access article distributed under the terms and conditions of the Creative Commons Attribution (CC BY) license (https://creativecommons.org/licenses/by/4.0/).

1. Introduction

Heat sealing is a fundamental process for creating effective closures in flexible polymer and biopolymer films, which is crucial for packaging applications. This process involves pressing two film layers between heated metal bars, allowing the polymer to melt and intermix via mass diffusion. Upon cooling, this interdiffusion and entanglement of polymer chains creates a strong, rigid bond. Seal strength, defined as the maximum force per unit seal width required to separate sealed materials, is a key indicator of seal quality. This strength is significantly influenced by the sealing temperature, applied pressure, and

dwell time, which is the duration for which the material remains in the heating zone [1]. Understanding the failure mode of a heat-sealed material, such as delamination, peeling, or tearing, is also vital for assessing packaging performance and the integrity of the sealed surface [1,2].

a- The Rise of Edible and Biodegradable Films

There is growing global interest in edible and biodegradable flexible films as sustainable alternatives to non-recyclable synthetic plastic packaging. These innovative films, especially those derived from starch, show great promise for packaging dry ingredients, preserving food quality, and even serving as active ingredient delivery systems within food processing [3,4]. Effective heat sealing is critical for their widespread use in bags and sachets, as the seal strength directly impacts their ability to withstand handling and storage [5].

While heat sealing has been explored for various biodegradable films, including blends of starch and other polymers (some synthetic), specific information on fully edible films remains limited. Research has focused on the sealing properties of whey protein and zein films, with zein demonstrating improved heat sealing capabilities. Carbohydrate and protein blends have also been evaluated for their seal strengths [5].

Despite these advancements, detailed reports on edible films primarily composed of starch are limited. Although heat-sealed banana flour films have been used for food packaging, comprehensive data on their seal strength are often lacking. To address this gap, recent research has focused on thoroughly evaluating the heat-sealing properties of edible films made from starch and functional polysaccharides. The latter are added to enhance mechanical and barrier properties, ultimately aiming for effective heat sealing in practical packaging applications [1].

b- Advancements in Bio-based Packaging Materials

Broader research on bio-based polymers and composites is crucial for developing sustainable alternatives to petroleum-based plastics and mitigating environmental pollution [6]. This research highlights the significant economic potential of producing biodegradable packaging from plant-based sources, offering a viable solution to plastic pollution, although large-scale implementation still faces challenges [7].

Various studies have pushed the boundaries of edible and biodegradable film technology.

- Corn starch and functional polysaccharides: Self-supporting edible films composed of corn starch and functional polysaccharides (amylose, methylcellulose, and hydroxypropyl methylcellulose) have been evaluated for heat sealing between 85 and 166 °C [1].
- Protein films: Although protein films are promising alternatives to conventional plastics, they often require improved mechanical and barrier properties through physical, chemical, or biochemical treatments. Combining nanotechnology with enzymatic and physical treatments appears to be the most promising approach for creating optimal protein packaging for diverse food applications [8].
- Starch with essential oils: Biodegradable corn/wheat starch films infused with lemon essential oil (LEO) and surfactants exhibit modified physical properties and significantly increased antimicrobial activity, making them potential biodegradable active packaging for controlling microbial food spoilage [9].
- Blends for enhanced properties:
    - Soluble soy polysaccharide (SSPS) and gelatin: Blended films of SSPS and gelatin have been developed to enhance heat sealability, strength, and stability, making them promising for rapidly dissolving packaging of powdered products [10].

- Cellulose acetate and nanofibers: A biodegradable bag for fish and meat was developed using cellulose acetate and cellulose nanofibers. This heat-sealable film, incorporating natural anthocyanin as an ammonia sensor, exhibited good properties and potential as an active biodegradable packaging with a freshness indicator [11].
- Starch-chitosan with graphene oxide: Biodegradable active films of starch-chitosan reinforced with reduced graphene oxide have shown improved functional properties while maintaining heat sealability for food packaging [12].
- Cassava starch with plasticizers: The optimization of glycerol/sorbitol ratios in cassava starch films demonstrated that a 1:1 ratio yielded the best strength and sealing morphology, emphasizing the importance of plasticizer combinations [13,14].

- Soy protein isolate with Tara pod extract: Biodegradable films made from soy protein isolate (SPI) and Tara pod extract (TPE) have demonstrated improved mechanical, UV/oxygen barrier, and heat-sealing properties, providing greater protection for fatty foods compared to polyethylene containers [15].
- HPMC/cellulose nanofiber films: Active, printable, and heat-sealable HPMC/cellulose nanofiber films containing propolis-loaded zein nanoparticles are emerging as environmentally friendly alternatives to plastics for food packaging [4].
- Vegetable purees and pectin: "Greek salad"-style edible films made from vegetable purees and pectin have demonstrated good heat-sealing properties, with future efforts focusing on optimizing the basic film for packaging fatty foods [16].
- Pectin with curcumin-loaded nanoparticles: Enhanced pectin-active films with curcumin-loaded phytoglycogen nanoparticles have improved barrier, antioxidant, and antibacterial properties, showing potential to replace heat-sealable plastics in oil packaging [17].
- Chitosan: This promising antimicrobial biopolymer is being explored for biodegradable packaging to extend food shelf life; however, further research is needed for optimal properties and commercialization [18].
- Rice biopolymer, chitosan, and alginate adhesive: A novel, nontoxic, and sustainable adhesive based on rice biopolymer, chitosan, and alginate has proven effective in bonding biopolymer surfaces with good strength, even under high-humidity conditions, offering a promising alternative for sealing bio-based films [19].
- Soy protein films with cow horn: Heat-sealable soy protein films reinforced with cow horn have been developed as smart (pH-sensitive) and environmentally friendly packaging materials with good mechanical properties and UV protection for food [20].
- Starch-Based Packaging: Despite significant advancements, starch-based packaging, although sustainable and affordable, faces practical challenges in large-scale implementation, particularly in developing countries with limited recycling infrastructure. These include issues related to industrial processing, storage, and moisture resistance [21,22]. Addressing these stages comprehensively is crucial for scaling up production and successfully replacing single-use plastics [23].

c- Exploring Chañar Brea Gum (CBG) in Edible Films

Chañar Brea gum (CBG), extracted and purified from *Parkinsonia precox*, is a water-soluble hydrocolloid whose solubility increases with temperature. Its solutions exhibit increased viscosity with higher CBG concentrations and lower temperatures, with pH also influencing viscosity [24]. CBG also functions as a stabilizer, emulsifier, foam former, and film former.

Research has focused on formulating CBG-based films and coatings using glycerol as a plasticizer. These films typically exhibit amber-colored transparency with a dense,

homogeneous microscopic structure. Glycerol addition increases the wetting capacity and water solubility (with temperature), while the water vapor permeability remains stable up to 20% glycerol before increasing. Glycerol also reduces the opacity and tensile strength of films [25].

Further investigations have explored the improvement of CBG film properties by adding montmorillonite (MMT). MMT incorporation reduced foaming in the film-forming solution. Films created by casting MMT exfoliates within the CBG matrix exhibited optical properties dependent on the nanofiller concentration. The addition of MMT decreased film solubility, moisture uptake, and water and gas permeability, while increasing the Young's modulus and tensile strength, albeit with a reduction in the elongation [26].

Water transport in edible films made of hydrophilic polymers is complex. Thermodynamic and phenomenological analyses of MMT nanoparticle incorporation into CBG films revealed that MMT makes the exothermic adsorption process less favorable, reducing water uptake. The changes in entropy and isosteric heat suggest a more stable and ordered structure in the MMT-containing films, with a lower affinity for water. The water vapor permeability of CBG films decreased with the addition of MMT due to increased tortuosity and reduced hydrophilicity [27].

CBG has also been used as an emulsifier and matrix component in edible whey protein concentrate (WPC) films with lipids (sunflower oil or beeswax) to enhance their water vapor barrier. Ultrasonication helped to achieve homogeneous emulsions. CBG effectively reduced emulsion droplet size, especially at lower lipid contents. While lipids decreased mechanical strength, their addition, enhanced by CBG, reduced water vapor permeability. Overall, CBG has proven to be a good emulsifier for lipids, improving the homogeneity and mechanical properties of WPC-lipid composite films [28].

Finally, bilayer films of pectin and CBG were formulated, and their properties were compared with those of single-layer films. Microscopic and surface observations confirmed the integrity of the bilayer films, without delamination. The high solubility of CBG influenced the solubility of the bilayer film. The water vapor permeability depended on the exposed layer during desorption, being lower than that of the CBG films alone but higher than that of the pectin films of similar thicknesses. The distinct properties of each layer make these bilayer films potentially interesting for applications like controlled drug release [29].

This paper presents a comprehensive evaluation of the heat-sealing capability of films developed from chañar brea gum, a biopolymer with potential for packaging high-value-added products. Heat sealability is a critical property in the packaging industry, as it directly determines the integrity and functionality of the final package, ensuring the protection of the product inside. The heat-sealing process involves the controlled fusion of the surfaces of two films through the application of heat and pressure, followed by cooling to solidify the bond. To fully understand this heat-sealing behavior and its underlying mechanisms, this study employs a battery of determinations that explore the fundamental properties of the films: proximate analysis, antioxidant capacity, FTIR, DSC, TGA-DTGA, XRD, mechanical testing, water vapor permeability and sorption, and biodegradability. By integrating the results obtained from all these analyses, this study seeks to evaluate and explain the "intimate relationships"—that is, the complex interconnections between the molecular structure, composition, thermal behavior, mechanical properties, and barrier properties of chañar brea gum films—and how these fundamental properties dictate and control their heat-sealability. This comprehensive approach is crucial for optimizing the heat-sealing process and designing functional and efficient biodegradable packaging in the food and pharmaceutical industries.

2. Materials and Methods

2.1. Raw Material

Chañar brea gum was collected by "Viva el Monte, Traslasierra, Argentina" from the exudate of the *Parkinsonia precox* tree located at 32°06′36.5″ S, 65°03′56.8″ W, named "La Travesía," Traslasierra, Córdoba, Argentina.

The procedure consisted of dissolving the exudate in distilled water and filtering it. The filtrate was precipitated with ethanol at a 70/30 ratio in distilled water. The mixture is filtered again, and the retentate is dried at 60 °C for 24 h [30–32].

The yield was calculated from 100 g of CBG using the following equation:

$$Yield\% = 100\frac{CBG_{sol}}{CBG} \quad (1)$$

where CBG is the initial mass (100 g) and CBG_{sol} is the mass of the resulting filtration processes [33].

2.1.1. Film Preparation

The films were prepared by adding 10 g of CBG to 100 mL of water, and 5 mL of glycerin was used as a plasticizer and molded in a box of 29 cm × 21 cm × 4 cm. The samples were then dried at 60 °C for 24 h. Finally, the product was unmolded and packaged in a self-sealing polyethylene bag [25,27].

2.1.2. Film Heat-Sealing

Heat sealing was performed on an OX400 bag sealer (Oryx, Shandong, China) at 140 °C, 3 mm wide, for 3 s. The samples to be heat-sealed were cut into rectangular strips of film, each 100 mm long and 20 mm wide. The strips were conditioned at 40% (RH) and a temperature of 25 °C for 24 h. For sealing, two conditioned strips were placed one on top of the other and sealed. Heat sealing was performed on 2 cm × 10 cm strips of chañar brea gum in the horizontal (CBG-H) and vertical (CBG-V) directions. The measurements were repeated three times. Seal strength was determined according to the ASTM F88-09 method (ASTM, 2009) [34] using a Brookfield CT3 texturometer (Middleboro, MA, USA). The maximum force (N) required to peel/tear the seal was recorded numerically and graphically, and the failure mode was simultaneously noted. The seal strength was calculated as the maximum force/film width [1].

2.1.3. Proximate Analysis of Biomass

Proximate analysis of the macerated biomass powder was performed according to AOAC standard methods (AOAC, 2012 [35]). The nitrogen content was measured using the Kjeldahl–Arnold–Gunning method, calculating total proteins with a 6.25 ± 0.22 factor (AOAC. 920.12); protein productivity (mg/L/h) was also determined. Total fat content was analyzed using the Soxhlet gravimetric method with petroleum ether (Sigma Aldrich, Saint Louis, MI, USA) (AOAC 945.39). Crude fiber analysis was performed using the digesting sample method with H_2SO_4 and NaOH (Sigma Aldrich) (AOAC 962.09). The ash content was determined by weight difference after calcining the sample (AOAC 945.46), and the moisture content was determined by heating under reduced pressure (AOAC 945.46). Carbohydrates were calculated indirectly as follows: total carbohydrates = 100 − (Proteins + Total Fat + Moisture + Ash). Following these standard procedures ensured accurate and consistent results, providing valuable data for research and industry [36].

2.1.4. Antioxidant Activity Assays

Reactive oxygen species (ROS), such as DPPH radicals, are the culprits behind oxidative damage and functional decline, notably affecting the liver. Given the detrimental impact of ROS, investigating novel polysaccharides as potential countermeasures is vital for developing effective treatments for liver damage and oxidative stress-related conditions in the future. Consequently, the determination (or measurement) of these harmful free radicals is a crucial prerequisite for evaluating such polysaccharides and uncovering their therapeutic potential. Research in this area, by studying the interaction between novel polysaccharides and ROS, holds promise for significant breakthroughs in healthcare and wellness [36].

Reducing Power

A reducing power assay was conducted to determine the reducing capacity of polysaccharide solutions, based on the method described in reference [36]. The execution of this method requires precision and careful incubation. The procedure involved adding phosphate buffer (2 M, pH 6.6), potassium ferricyanide (1% wt.), and trichloroacetic acid (10% wt., 2.5 mL) to halt the reaction. Subsequently, ferric chloride (0.2 mL) was added, and the absorbance was measured at 700 nm. To ensure reliability, the assay was conducted in triplicate, incorporating gallic acid as a positive control. The outcomes were presented as meq/mL of gallic acid, reflecting a rigorous approach to the assessment of reducing power.

DPPH Scavenging Activity

To determine the DPPH radical scavenging activity of polysaccharide solutions, a method based on a previous study [36] with some adjustments was employed. The protocol involved combining volumes of CBG solution (tested across a range, such as 0.1 to 1 mL) with a 90% ethanolic DPPH solution (0.15 M). Following a 30-min incubation period protected from light, the absorbance was recorded at 517 nm. The total antioxidant content was quantified as a percentage of antioxidant activity (% AA) using the following equation:

$$AA(\%) = \frac{(Ac - (Am - Ab))}{Ac} \times 100 \quad (2)$$

Following absorbance measurements, calculations were performed using a formula incorporating the absorbance of the control (A_c), sample absorbance (A_m), and blank absorbance (A_b). The entire procedure was performed in triplicate to ensure robust reliability. Ascorbic acid was used as a positive control, and a calibration curve was constructed based on the measurements of ascorbic acid standards. This calibration curve allowed the results to be expressed as mg/mL equivalents of ascorbic acid. Such meticulous measurements and subsequent computations have provided valuable insights into the antioxidant properties and potential health benefits of polysaccharides [36].

Total Polyphenol Content

Total phenolic compounds were determined using the Folin–Ciocalteu method [36–38], with modifications to enhance accuracy and precision. The protocol involved carefully combining a 5 mL CBG aliquot with 1.5 mL of Folin–Ciocalteu reagent (2 N) and 15 mL of 15% Na_2CO_3 solution in a volumetric flask. The volume was then adjusted to 25 mL using distilled water. The resulting solution was incubated for 2 h at room temperature, protected from light to allow the reaction to complete. The absorbance was measured at 760 nm. For quantification, a calibration curve was established using gallic acid (GA) as a reference standard, with six concentrations ranging from 1 to 6 mg/L being prepared

and measured. The entire analytical procedure was meticulously repeated to confirm the reproducibility and reliability of the data.

2.2. Fourier-Transform Infrared Spectroscopy

In this study, Fourier transform infrared spectroscopy (FTIR), a common technique in analytical chemistry for identifying chemical compounds, was used. The spectra were obtained using a Nicolet PROTEGE 460 spectrometer (Madison, WI, USA) in two modes: diffuse reflectance (DRIFTS) and transmission. Data collection was performed in the 700–400 cm^{-1} range by scanning each sample 64 times to ensure accurate results. The combined use of both modes allowed for a, detailed analysis of the chemical composition, structure, and molecular vibrations of the samples, ensuring the robustness and reliability of the obtained spectra for meaningful interpretation [39].

2.3. X-Ray Diffraction (XRD)

X-ray diffraction (XRD) studies were performed using an advanced Rigaku ULTIMA IV type II instrument (Tokyo, Japan). This instrument employed a Cu Kα lamp with a wavelength (λ_B) of 1.54 Å and a nickel filter for accurate measurements. Scanning was performed in the 2θ range from 3° to 60°, operating the equipment at 30 kV and 20 mA. Data collection was performed continuously at a speed of 3° per minute and a reading step of 0.02°. The average (triplicate measurement) interlaminar distance ($d_{spacing}$) was calculated using the Bragg equation.

$$d_{spacing} = \frac{n\,\lambda_B}{2sin\theta_B} \quad (3)$$

where $d_{spacing}$ represents the interplanar distance, θ_B refers to Bragg's angle, n is an integer value determined through analysis, and λ_B denotes the X-ray wavelength used [40].

$$I_{cr} = 100\,\frac{I_{max} - I_{ad}}{I_{max}} \quad (4)$$

The crystallinity index (I_{Cr}) was calculated from the normalized diffractogram. For this purpose, the intensities of the peaks corresponding to the lattice planes were used, such as the (110) reflection (I_{max}), observed around 21°, which represents the maximum intensity. The intensity of the amorphous diffraction (I_{ad}), taken at approximately 15°, was also used, following methodologies described in the previous literature [40,41], to determine I_{Cr}.

2.4. Differential Scanning Calorimetric Analysis (DSC)

Differential scanning calorimetry (DSC) was performed using a STA 449F3-Jupiter (Selb, Germany). Approximately 5 mg of the biopolymer sample was placed in an alumina crucible and heated from 25 °C to 400 °C at a constant rate of 5 °C/min This process was carried out under a dynamic nitrogen atmosphere with a flow rate of 25 mL/min, which was selected to accurately analyze the thermal behavior, characteristic transitions, and stability of the biopolymer [42].

2.5. Thermogravimetric Analysis

The thermal stability of the polysaccharide films was determined by thermogravimetric analysis (TGA) using a TA Instruments TG 295 analyzer (New Castle, DE, USA). Samples of approximately 8 mg were heated at 10 °C/min under a pre-filtered N_2 (99.99%) atmosphere with a flow rate of 50 mL/min using empty aluminum crucibles as references. Temperature calibration was performed using indium (melting point 156.60 °C) and the Curie point of Ni (353 °C) [43].

2.6. Scanning Electron Microscopy (SEM)

The film morphology was meticulously analyzed using a LEO 145VP scanning electron microscope (SEM), complemented by energy dispersive X-ray (EDAX) analysis using an EDS Genesis 200 (Jena, Germany). For SEM observation, the samples were prepared by immersion in liquid nitrogen and gold coating. Analyses were performed under high vacuum, with EDAX spectra obtained at an accelerating voltage of 120 kV to ensure accurate data collection of the elemental composition [44].

2.7. Mechanical Tests

The mechanical properties of the materials were evaluated using a Brookfield CT3 (Middleboro, MS, USA) instrumentaccording to ASTM D882 [45]. The tests were performed in triplicate at 25 °C and 40% relative humidity, with a constant tensile rate of 0.1 mm/min. Samples of 40 mm length and 10 mm width were used, and the thickness of each film was measured using a micrometer. The force (F) and strain (Δl) data were recorded until failure. The tensile strength (σ) was calculated as the maximum load divided by the initial cross-sectional area (A), the percentage elongation at break (% ε) as the percentage change from the initial length (l = 40 mm) at failure, and the elastic modulus (E) as the slope of the stress (σ) vs. strain (ε) curve in the linear elastic region [44,46].

$$E = \frac{\sigma}{\varepsilon} \tag{5}$$

$$\sigma = \frac{F}{A} \tag{6}$$

$$\varepsilon = \frac{\Delta l}{l_0} \tag{7}$$

2.8. Water Vapor Permeability

Water permeability was determined using Electrotech Systems equipment that controlled the temperature and humidity in a closed system. Weight change was recorded using a RADWAG balance (Radom, Poland) accurate to 0.1 mg, and the film thickness was measured using a Kolfe micrometer (Mahr, Germany) accurate to 0.1 mg. Circular film samples (25 mm in diameter) with measured thicknesses were placed in the perforated caps of bottles containing 20 g of silica gel. The sealed bottles were maintained at 30 °C and 85% relative humidity, and weight changes were recorded according to a detailed schedule for 24 h in triplicate, following ASTM E96 [47].

$$\tau = \frac{Q}{t\ A} \tag{8}$$

$$P = \frac{\lambda}{\Delta P}\ \tau \tag{9}$$

where τ is the transmission speed (ng/m^{2}s), ΔP is the pure water vapor pressure (4238.605 Pa), t is the measurement time(s), Q is the permeating mass (ng), λ is the thickness of the film (m), and A is the area of the cell (m^2) [46–48].

2.9. Biodegradability

Biodegradation is the breakdown of biopolymers by microbial enzymes (bacteria, yeast, and fungi), which can be total (generating methane or CO_2) or partial (changing composition/properties). A recent study evaluated the biodegradation rates in a container covered with moistened soil (80% RH, 25 °C) for 30 days. The test was performed in triplicate on 2 cm × 4 cm strips of chañar brea gum with horizontal (CBG-H) and ver-

tical (CBG-V) heat seals, and the strip was not heat-sealed (CBG). Biodegradability was determined by the weight change between the initial samples as a function of time. These findings improve our understanding of biodegradation mechanisms and their implications for sustainable waste management [46,48].

3. Results

3.1. Proximate Analysis of Biomass and Antioxidant Capacity

Starting with 100 g of chañar brea exudate, an extraction process was carried out to obtain purified chañar brea gum (CBG), achieving highly efficient extraction. The specific yield achieved during the operation was 82.33 ± 2.45%. This means that the vast majority of the initial exudate can be converted into gum. This yield underscores the effectiveness of the extraction method used. The analyzed product exhibited notable antioxidant and bioactive properties, evidenced by a DPPH value of 9.81 ± 0.32 meq/L ascorbic acid equivalent. The polyphenol content was 1.16 ± 0.034 meq/g of gallic acid, quantified using the Folin–Ciocalteu method. In addition, it demonstrated a hydroxyl radical (OH*) scavenging capacity of 4.2 ± 0.25% and a reducing power of 4.89 ± 41 meq/g, which underscores its potential activity. Its nutritional composition is characterized by a high carbohydrate content, constituting 86.97 ± 3.77% of its weight. It provides moderate protein content (6.36 ± 023%) and is significantly low in total fat, representing only 1.19 ± 0.03%. Other components analyzed included 4.07 ± 0.15% ash, 3.12 ± 0.11% moisture, and an extremely low sodium content of 0.0114 ± 0.002%. Similar results have been reported for pectin, *Lithraea molleoides* gum, and Geoffrea decorticans Chañar gum [33,49]. No changes were observed in the proximal analysis and antioxidant capacity of the heat-sealed CBG films.

3.2. X-Ray Diffraction (XRD)

Data obtained through techniques such as X-ray diffraction (XRD) are essential for characterizing these polysaccharides, even though they are predominantly amorphous. These data, particularly $d_{-spacing}$, allow us to infer crucial information about the intermolecular distances between polymer chains, as well as to identify structural modifications induced by environmental changes such as moisture content or temperature fluctuations. Understanding this structure at the molecular level is vital for developing new materials with improved functionalities. In the context of the packaging industry, modulating these structures can translate into the creation of films with superior barrier properties against gases such as oxygen, thus significantly extending the shelf life of food products that come into contact with them [50].

Amorphous polysaccharides are fundamental components of numerous natural and synthetic materials. Therefore, a thorough understanding of their structural properties is essential in diverse fields, including pharmaceuticals, food science, and materials engineering. X-ray diffraction (XRD) is a key analytical technique for this purpose. Although amorphous polysaccharides do not exhibit sharp peaks characteristic of crystalline materials, their XRD patterns provide valuable information about the arrangement and organization of their molecular chains. The analysis of these diffuse patterns, including their numerical characteristics, serves as a basis for describing the structure and properties of these polysaccharides. Comparing these diffraction patterns with standard references or known structures of related compounds or polymers provides important details about their arrangement at the atomic and molecular levels, even in the absence of long-range crystalline ordering [50].

The X-ray diffraction (Figure 1) results for the CBG film revealed significant differences in its molecular structure after heat sealing, see Table 1. Initially, the heat-sealed film exhibited a $d_{-spacing}$ value of 4.88 nm and a crystallinity index of 34.16%. The $d_{-spacing}$,

which represents the distance between atomic or molecular planes within the crystalline structure of the material, suggests a certain level of organization in the polymer chains. In contrast, the crystallinity index indicates the percentage of the material that exhibits an ordered, crystalline structure compared to the amorphous and disordered fractions [51]. No changes were observed in the DRX patterns of the heat-sealed CBG-H and CBG-V films.

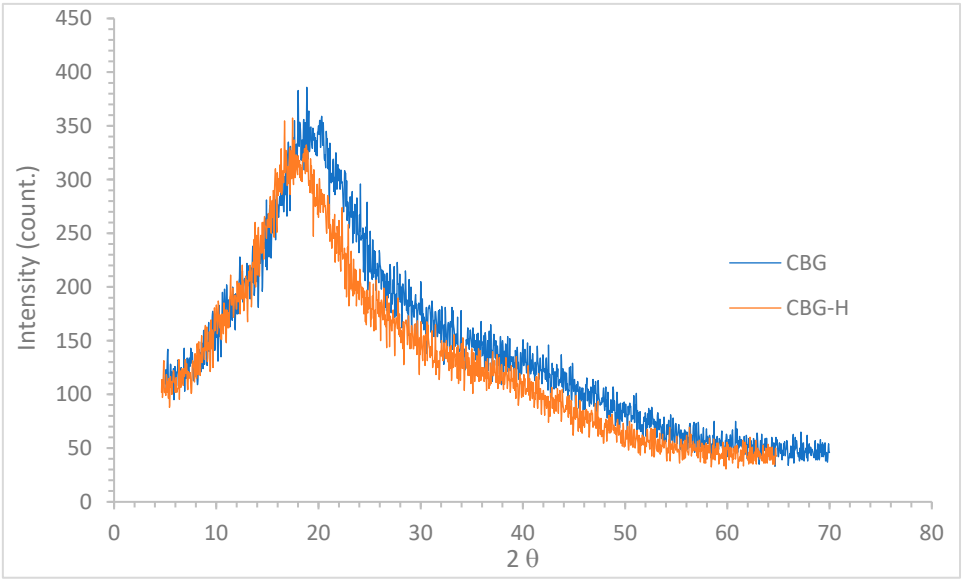


Figure 1. XRD of CBG and CBG-H.

Table 1. XRD data of CBG and CBG-H.

Flour	2θ	$d_{spacing}$ (nm)	I_{Cr} %
CBG	18.15 ± 0.72	4.88 ± 0.97	34.16 ± 0.97
CBG-H	19.05 ± 0.84	4.66 ± 0.91	32.54 ± 0.89

After applying the heat-sealing process of CBG-H, the XRD results showed a decrease in both parameters. The d-spacing was reduced to 4.66 nm, and the crystallinity index decreased to 32.54%. This shrinkage in d-spacing could be interpreted as a rearrangement of the polymer chains to a slightly smaller interlayer distance, possibly induced by the thermal energy applied during the heat sealing. The decrease in the crystallinity index suggests that the heat treatment caused a slight loss of the ordered structure in favor of a more amorphous phase [52].

This reduction in crystallinity after heat sealing is not a universal phenomenon for all polymers, as it depends on the specific nature of the material and the process conditions. However, in some cases, partial melting or thermal stress during heat sealing can alter existing crystalline regions or hinder the formation of new ordered structures during cooling, leading to a net decrease in the crystallinity. These changes in the nanostructure of the CBG film, evidenced by the variation in $d_{-spacing}$ and crystallinity index determined by XRD, are crucial to understanding how heat sealing affects the physical and mechanical properties of the material, such as its barrier, flexibility, or sealing strength [53].

The chitosan film presented two distinctive peaks at 10.46° and 20.1° (2θ), typical of its semi-crystalline nature [54]. Carboxymethylcellulose (CMC) [55] exhibited a characteristic peak at 20.71° (2θ), reflecting its structure with a degree of ordering, although probably lower than that of native cellulose due to substitution. Materials designated CBG and CBG-H showed peaks at 18.15° and 19.05° (2θ), suggesting the presence of specific crystalline structures. In contrast, a study on sonicated spores of *Ganoderma lucidum* [56]

revealed a significant impact of physical treatment. These spores lost their original chitosan morphology, experienced a dramatic decrease in their degree of crystallinity (shifting toward a more amorphous state), and showed an increase in the degree of deacetylation of the constituent chitosan. Taken together, the XRD results demonstrate how the technique allows for the identification of crystalline structural features of different polymers and biological materials, which can contribute to the disruption of crystallinity [52].

3.3. Fourier-Transform Infrared Spectroscopy (FTIR)

Analysis of the infrared spectrum (Figure 2) revealed prominent absorption bands linked to specific functional groups. The –OH stretching band at 3430 cm^{-1} indicates the presence of hydroxyl groups. C–H stretching occurred at 2920 cm^{-1}, and a general carbonyl band was present at 1740 cm^{-1}. More specifically, the carboxylate group exhibited a characteristic carbonyl band at 1640 cm^{-1} (C=O from $–COO^-$). Bending vibrations from the–CH_2OH side chains produced multiple bands at 1420 cm^{-1} and 1380 cm^{-1}. A strong peak at 1250 cm^{-1} is assigned to the C–O–C stretching. C–O glucopyranosic bending is observed around 1040 cm^{-1}, and a signal at 890 cm^{-1} may suggest the presence of a C-N bond. Out-of-plane C–O bending vibrations were detected at 775 cm^{-1} [46,49]. Together, these assignments provide a detailed picture of the structure of the compound. No changes were observed in the FTIR spectra of the heat-sealed CBG films.

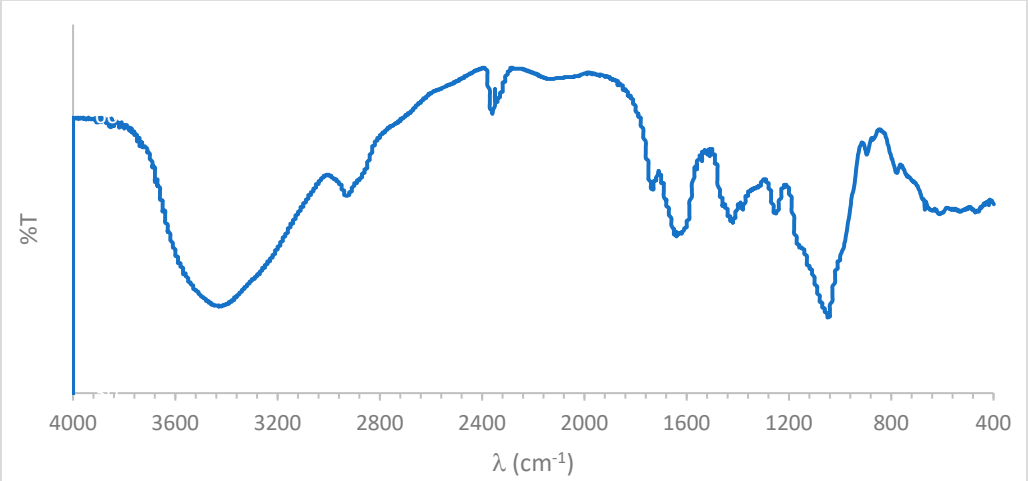


Figure 2. FTIR of CBG.

3.4. Differential Scanning Calorimetry (DSC)

Differential Scanning Calorimetry (DSC) analysis of CBG provides essential information about its thermal transformations, as shown in Figure 3. The DSC analysis initially revealed a clear glass transition (T_g) at 43.78 °C. This second-order transition marks the point at which the amorphous regions of the CBG transition from a rigid, glassy solid state to a more flexible, rubbery state with greater molecular mobility. T_g is a critical parameter for predicting the behavior of amorphous materials, affecting their mechanical stability, reaction kinetics, and diffusion characteristics. An endothermic peak was observed around 75.85 °C, associated with an enthalpy of 216.2 J/g. The endothermic nature of this energy-intensive event, combined with its temperature, strongly suggests the desorption or elimination of potentially adsorbed water from the sample. The presence of moisture, even in small amounts, can significantly influence the T_g and stability of CBG, making this peak relevant for understanding its behavior under different ambient humidity conditions.

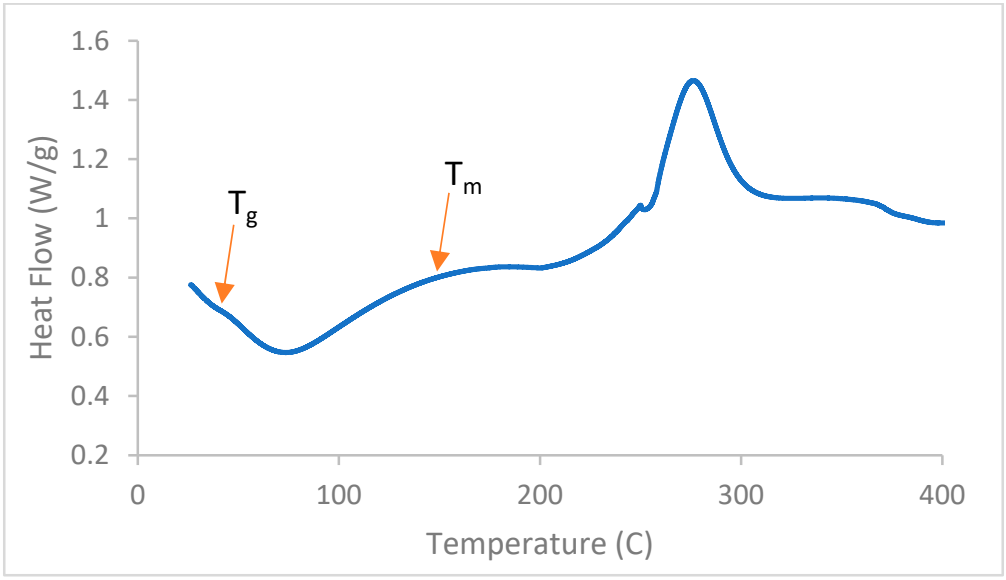


Figure 3. DSC of CBG.

As the temperature continued to increase, the DSC displayed a prominent first-order phase transition: the melting peak (T_m) at 152.48 °C. This pronounced endothermic peak represents the energy absorbed during the melting of crystalline CBG, transforming it from a solid to a liquid. The melting temperature is an intrinsic property of crystalline substances and a key indicator of their purity. Finally, at a higher temperature of approximately 275.39 °C, another significant endothermic peak appeared with an area of 369.9 J/g. This high-temperature thermal event, which also requires the absorption of a considerable amount of energy, is indicative of CBG degradation or thermal decomposition processes. The temperature at which this decomposition peak occurs is critical for determining the thermal stability of the compound and establishing safe temperature limits for its processing and long-term storage, ensuring that CBG maintains its chemical integrity and potency. A similar discussion for different biodegradable film materials can be found in reference [56,57].

3.5. Thermogravimetric Analysis (TGA-DTGA)

According to the TGA and DTGA analyses of CBG, it demonstrated thermal stability up to approximately 200 °C. Below this temperature, both materials exhibited minimal mass loss, indicating the absence of significant degradation or evaporation of the volatile components. Above 200 °C, the TGA and DTGA begin to show more pronounced mass losses, as shown in Figure 4. This suggests that CBG maintains its structural integrity and composition up to this temperature limit. Therefore, 200 °C represents a critical point in its thermal behavior before decomposition processes begin, where the reference [58] provides a thermal stability value of less than 250 °C.

3.6. Scanning Electron Microscopy (SEM)

Figure 5 shows a scanning electron microscopy (SEM) image of the cross-section of a heat-sealed chañar brea gum (CBG-H) film. In this micrograph, the heat-sealed area of the CBG-H film is clearly visible, appearing well-defined, allowing the area where heat was applied to seal to be visually distinguished. The heat-seal joint does not show any cracks and is almost quasi-homogeneous, with very few holes or gaps. This phenomenon occurs when two surfaces of the same material are heat-sealed, leaving some air pockets that become evident as gaps.

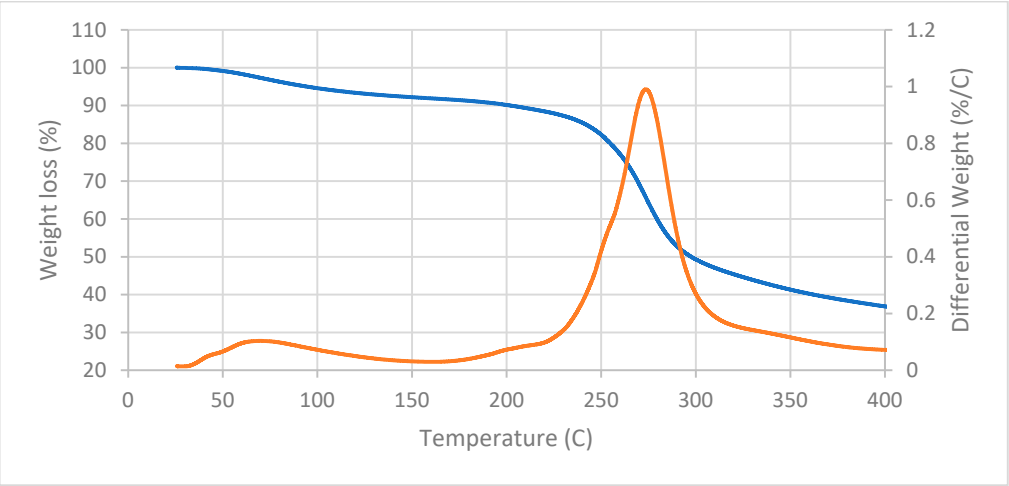


Figure 4. TGA (blue) and DTGA (orange) of CBG.

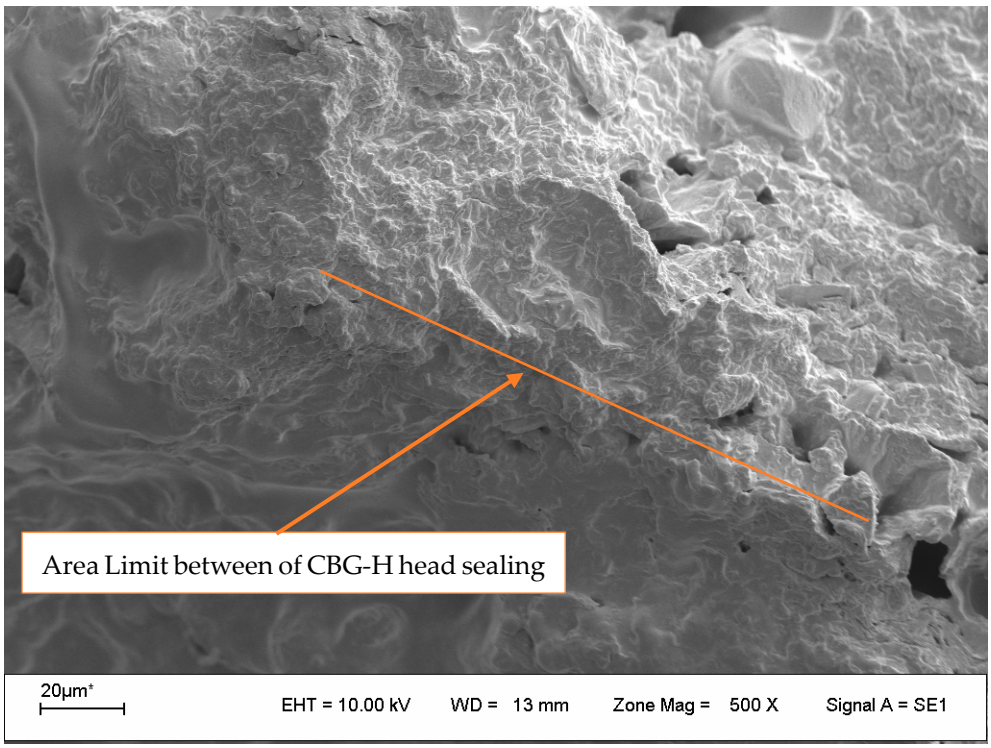
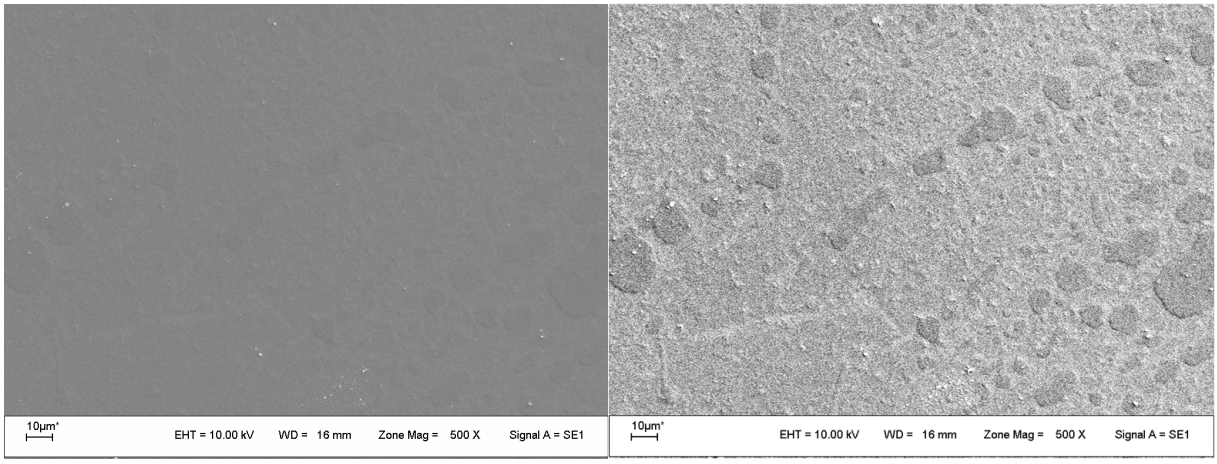


Figure 5. Cross-section of the CBG-H film. * in microns.

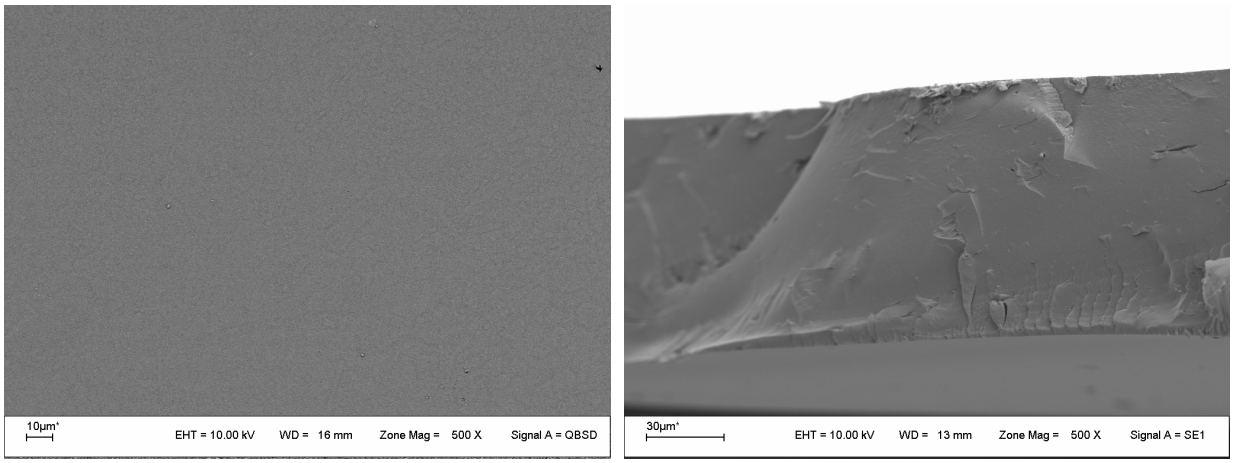
The surface image of the heat-sealed film offers a detailed view of its surface morphology (see Figure 6a). A general gray background, which is characteristic of the base material, was observed. Against this relatively uniform background, certain shadows with a more rounded morphology were observed. These shadows appear as alterations in the surface texture or topography of the heat-sealed area. For clear identification and visual reference, these specific areas, which correspond to the section where heat was applied to perform the seal, are indicated by arrows. The appearance of these rounded shadows, unmistakably indicated by the arrows on the gray background of the film, precisely and clearly delimits and shows the specific section that was subjected to the heat-sealing process, allowing it to be differentiated from the rest of the film surface (Figure 6b).



(**a**) (**b**)

Figure 6. (**a**) Surface SEM image of the heat-sealed CBG-H film. (**b**) 90% de contrast. * in microns.

According to the analysis of images obtained by scanning electron microscopy (SEM), both in cross-section and surface view (Figure 7a), the chañar brea gum (CBG) film that was not heat-sealed exhibited distinctive structural characteristics, similar to the reference [25,59]. The cross-sectional image allows for an in-depth observation of the internal organization of the material (Figure 7b). In this regard, the absence of large pores, significant cavities, or noticeable internal separations suggests a compact and dense structure. At the same time, the surface image provides information on the texture and uniformity of the outer layer of the film. In both perspectives, homogeneity is evident; the micrograph presents a uniform appearance along its length without showing clearly separated distinct phases, irregular accumulations of material, or abrupt variations in density or surface texture. This dense and homogeneous structure observed both on the surface and inside the non-heat-sealed CBG film indicates a uniform distribution of its components and robust internal cohesion before any localized heat treatment, such as heat sealing.



(**a**) (**b**)

Figure 7. (**a**) Surface image of the CBG film without heat sealing. (**b**) Transversal cut. * in microns.

3.7. Water Sorption and Water Vapor Permeability

A comparison of the water vapor interaction properties of standard chañar brea gum (CBG) and horizontally heat-sealed chañar brea gum (CBG-H) revealed notable differences. The standard CBG sample exhibited a water vapor sorption rate of 3.40 g/g, indicating a high capacity to absorb moisture from the environment. In contrast, horizontally heat-

sealed chañar brea gum (CBG-H) exhibited a significantly lower sorption rate of only 1.16 g/g. This difference suggests that the heat-sealing process drastically reduces the affinity of the material for water.

Similarly, the water vapor permeability differs substantially. The standard CBG exhibits a permeability of 1.70 ng m/(m^2 s Pa), implying that water vapor passes through the film with relative ease. In contrast, horizontally heat-sealed CBG-H had a much lower permeability of 0.37 ng m/(m^2 s Pa). This demonstrates that horizontal heat sealing provides the film with a much more effective barrier against water vapor penetration.

Considering these findings in conjunction with other possible effects of heat-sealing, such as a potential reduction in water sorption capacity (absorption/adsorption), these data indicate that the horizontal heat-sealing treatment significantly and quantifiably improves the moisture barrier properties of the Chañar Brea gum film. The combination of lower sorption and such a significant reduction in water vapor permeability positions the CBG-H film as a considerably more promising and suitable material for use in various applications where actively controlling moisture transfer is crucial, such as packaging for moisture-sensitive products, protective coatings, or components in products requiring dry environments. For a more in-depth discussion, refer to [60].

3.8. Mechanical Test and Heat-Sealing Capacity

A thorough comparison of the mechanical properties of chañar brea gum (CBG) films revealed that both the initial film thickness and heat-sealing method employed considerably influenced their performance under tension (Table 2). A marked difference was observed when analyzing the maximum elongation at break, a key indicator of the material's flexibility and stretchability before failure. The CBG sample with a thickness of 190 microns exhibited a significantly lower maximum elongation of only 5.11%. This contrasts markedly with the heat-sealed samples, where CBG-H (horizontally heat-sealed) reached 11.09% and CBG-V (vertically heat-sealed) reached 12.13%. This disparity suggests that either the base film used for heat sealing is inherently more extensible or the heat sealing process itself induces structural changes that increase the ductility of the film in the analyzed area, allowing it to deform significantly more before breaking compared to the standard film of lower thickness.

Table 2. Films' mechanical test.

Film	e (μm)	ε_{max}%	τ_{max} (MPa)	E (MPa)
CBG	190	5.11	4.48	132.0
CBG-H	307	11.09	3.36	96.8
CBG-V	305	12.13	4.58	159

Regarding the ultimate tensile strength, which quantifies the maximum tensile force that the material can withstand before fracturing, the values also vary between samples (Table 2). The CBG film with a thickness of 190 μm has an intermediate value of 4.48 MPa. The CBG-H sample recorded the lowest ultimate tensile strength of the group, at 3.36 MPa with a thickness of 307 μm, which could indicate some weakness induced by horizontal heat sealing. In contrast, the CBG-V proved to be the most tensile, reaching 4.58 MPa, slightly surpassing even the 305 μm sample. This suggests that vertical heat sealing, unlike horizontal heat sealing, appears to maintain or even slightly improve the material's inherent resistance to tensile fracture.

Finally, when Young's modulus, a measure of stiffness or resistance to elastic deformation under stress, was examined, clear differences were evident. The 190 μm CBG sample had a modulus of 132 MPa, placing it at an intermediate stiffness within the group. The

CBG-H sample, with a modulus of 96.8 MPa, was noticeably less stiff, consistent with its greater elongation and lower tensile strength; it was a "softer" or more flexible material. In contrast, the CBG-V sample exhibited the highest Young's modulus (159 MPa), indicating that it was the stiffest and most resistant to initial deformation under load.

In summary, these results show that both the original film thickness (comparing 190 μm with CBG-H and CBG-V) and, crucially, the heat-sealing orientation (horizontal versus vertical) have a significant impact on the mechanical profile of the chañar brea gum films. The 190 μm film was less extensible but had intermediate strength. Horizontal heat sealing (CBG-H) resulted in a more flexible material (higher elongation, lower modulus) but was less resistant to breakage (lower tension). Surprisingly, the vertically heat-sealed sample (CBG-V) appears to optimize the properties, combining high stretchability (elongation comparable to CBG-H) with the highest break strength and stiffness. This positions it as the option with the most robust and balanced mechanical profile among the samples analyzed, suggesting that vertical heat sealing is an effective process for obtaining CBG films with improved performance for applications requiring strength, stiffness, and a certain degree of flexibility. Similar details can be found in references [25,61].

Heat Sealing Capacity

The ultimate goal of films developed from chañar brea gum (CBG) is to use them as packaging materials. Therefore, evaluating their heat-sealing capabilities is critical and indispensable aspect. Heat sealing is the fundamental mechanism for creating hermetic seals and ensuring package integrity, and its quality directly determines the protection offered by the package to the product it contains [62].

In this context, the mechanical behavior of CBG films subjected to heat sealing was analyzed, specifically evaluating the strength and failure modes of the seal. During the tensile tests applied to the sealed samples, it was consistently observed that the predominant failure mode was not the separation or opening of the heat-sealed area, but rather fracture due to tearing of the film material adjacent to the seal line. This finding is of utmost importance as it highlights the inherent strength of the heat seal compared to the mechanical strength of the unsealed film in that region. The film yield before the seal indicates that the bond formed by the heat seal is more resistant to the applied forces than the film itself, which is a key criterion for a high-quality seal in packaging applications [62].

In this work, the tensile tests yielded seal strength values of 656 N/m for CBG-H and 950 N/m for CBG-V. Similar results were obtained with potato starch films containing halloysite nanoclay, which had good heat sealability and a seal strength of approximately 500 N/m, comparable to that of synthetic films (>600 N/m) [62]. Other similar results were obtained for whey protein isolate/lipid emulsion edible films [63] and starch films filled with nanoparticles [64].

Considering that the functionality and reliability of a package crucially depend on the integrity of its closure, the goal is to achieve a "good seal." An optimal seal is achieved at the microscopic and molecular levels, implying that, under the controlled action of heat and pressure, the interfaces between the individual layers of the film being joined effectively disappear. This occurs because of sufficient molecular interactions between the polymer chains of both surfaces, promoting their interdiffusion and the formation of a new, homogeneous, continuous layer in the bonded area. This molecular fusion results in an internal cohesion in the sealed region that is ideally as strong as or stronger than that of the base material. The evidence observed in the mechanical analysis, where the film failed before the seal, suggests that the heat-sealing process applied to CBG films achieved precisely this successful fusion, resulting in a seal with a strength superior to

that of the base material, thus fulfilling a fundamental requirement for its potential use as packaging [65,66].

Heat sealing is another critical factor, along with the barrier and mechanical properties of the material developed for food packaging. A good seal must be strong enough to keep the product in the package and airtight enough to keep the product fresh throughout its shelf life, such as cellulose films [67], wheat gluten [68], fish gelatin/ZnO nanorods [69], potato starch/halloysite nanoclay [61], pullulan (PUL)/soluble soybean polysaccharide [67], Tara pod extract/soy protein isolate [15], tapioca, and potato starch [70].

The heat-sealing properties of self-supporting edible films based on corn starch and functional polysaccharides (amylose, methylcellulose, or hydroxypropylmethylcellulose) were evaluated. The highest sealing strength was obtained at 166 °C, reaching values of 0.396 N/mm for the film containing amylose, 0.211 N/mm for the film containing methylcellulose, and 0.385 N/mm for the film containing hydroxypropylmethylcellulose [1].

Reference [10] emphasizes the importance of adequate sealing strength for the integrity of soluble soy polysaccharide packaging with gelatin. Comparative analysis revealed that the pure soluble soy polysaccharide film exhibited significantly lower strength (50 N/m) than the pure gelatin film (590 N/m). The incorporation of gelatin into blends with soluble soy polysaccharides significantly increased the sealing strength (up to 640 N/m with 60% gelatin), which was attributed to the differences in the composition and structure of the materials.

Biodegradable films were prepared by incorporating tara pod extract (TPE) into soy protein isolate (SPI) as the polymer matrix. TPE-SPI composite films exhibited improved mechanical properties, UV blocking, good heat sealing performance, and barrier properties [15].

According to reference [70], developed biodegradable edible films from tapioca (T) and potato (P) starch in various proportions, heat sealing is analyzed, it presented the lowest tensile strength and greatest elongation.

A paper [11] evaluated the characterization of cellulose acetate-CNF composite films and showed that the tensile strength decreased with increasing nanofiber concentration.

According to reference [12], the pure starch film showed low strength (0.06 N/mm), possibly due to its low polymer concentration. The combined addition of 75% starch and 25% chitosan resulted in the highest strength (0.17 N/mm), suggesting that chitosan at this ratio acts as a plasticizer, enhancing molecular interdiffusion during sealing via hydrogen bonding. However, increasing the chitosan ratio decreased the strength due to its lack of thermoplasticity. The incorporation of reduced graphene oxide reduced the strength to less than 0.04 N/mm, making sealing more difficult by restricting the mobility of the polymer chains and affecting hydrogen bonding. The common failure mode was peeling, which was indicative of sealing below the melting point of the polymer.

3.9. Biodegradability

The biodegradability of films made from polysaccharides is one of their most notable properties and one of the main reasons for their growing interest as an alternative to conventional plastics. Polysaccharides are widely available, renewable, and crucially susceptible to degradation by microorganisms present in various environments [71].

The biodegradation process of polysaccharide films involves the breakdown of polymer chains into simpler compounds, such as carbon dioxide, water, methane (under anaerobic conditions), and biomass, through enzymatic mechanisms carried out by bacteria, fungi, and other microbial communities. These enzymes, such as amylases (for starch), cellulases (for cellulose), and chitinases (for chitin/chitosan), hydrolyze the glycosidic bonds that link the monomeric sugar units in polysaccharides [72].

In general, polysaccharide films offer a sustainable alternative to petroleum-derived plastics due to their ability to be reincorporated into the natural cycle through biodegradation, contributing to the reduction of plastic waste accumulation in the environment. However, it is important to consider that the speed and extent of biodegradation can vary significantly depending on the specific film formulation and the conditions of the disposal environment [71,73].

Several factors influence the speed and degree of biodegradation of polysaccharide films, as described below. 1—Polysaccharide Type: The chemical structure and complexity of the base polysaccharide affect its susceptibility to enzymatic degradation. Polysaccharides, such as starch, tend to degrade more rapidly than crystalline cellulose. 2—Film Structure and Composition: The crystallinity of the polymer, its molecular weight, and the presence of chain branches influence the accessibility of enzymes to degradable bonds. 3—Additives and Plasticizers: The addition of plasticizers (such as glycerol) to improve flexibility can, in some cases, increase the rate of biodegradation by facilitating water absorption and increasing microbial activity. However, other additives may have opposite effects. 4—Environmental Conditions: Factors such as temperature, humidity, pH, oxygen availability, and the activity of microbial populations in the environment (soil, compost, and water) are crucial in determining the rate of degradation. Warm, humid environments with rich microbial activity generally accelerate this process. 5—Film Thickness: Thinner films tend to degrade faster due to a greater contact surface area available for microorganisms and enzymes [71,73,74].

Common polysaccharides used in the production of biodegradable films include

- Starch: Widely studied and used due to its low cost and availability. Thermoplastic starch films are biodegradable in various environments [74].
- Cellulose and its derivatives: Cellulose, the most abundant natural polymer, is an important base for biodegradable films. Its derivatives, such as carboxymethylcellulose or cellophane (regenerated cellulose), are also biodegradable [75].
- Chitin and Chitosan: Obtained mainly from crustacean exoskeletons, these polysaccharides have interesting properties for films, including biodegradability in the presence of chitinases [76].

In this work, CBG, CBG-H and CBG-V films are completely degraded after 4 days and, for example, similar studies of materials biodegradability are: heat-sealed arabinogalactan (AG) and poly (vinyl alcohol) (PVA) films with and without vinyllin [77], heat-sealed cellulose/zein films [75], films of oxidized sucrose (starch), chitosan, calcium chloride (alginate) and blends (starch/chitosan and starch/alginate, respectively) [74], edible films based on corn starch [74] and a functional polysaccharide, such as amylose, methylcellulose or hydroxypropylmethylcellulose (HPMC) [1], FucoPol films [76], chia mucilago films [78], Chañar films [48], Lithraea molleoides gum films [33], Pachycymbiola brasiliana gum films [44], alcayota gum films [43], Tragacanth films [49], Tara gum films [79,80], pectins films [46,81], etc. The connection between these biodegradable materials and the films presented in this work is that they are in the time range of 3 days to 3 months, which is the most important factor to consider when selecting materials applicable to environmentally friendly and non-polluting industrial demand.

4. Discussion

The data discussed in this section offers a comprehensive view of the potential of chenar gum as a biopolymer for the development of packaging materials, specifically through the heat-sealing technique. The discussion focuses on the interrelationship between the molecular structure, thermal properties, film morphology, and mechanical and barrier performance of the sealed material.

CBG is a polyarabinoglucuronoxylan [82] with an exceptionally high molecular weight of 1,890,000 g/mol [30]. This high molecular weight is a key factor, as it suggests the presence of long polymer chains that can generate a high degree of crosslinking. Such crosslinking is essential for the formation of cohesive and resistant films, providing a robust structural matrix that is a prerequisite for good mechanical performance. The chemical nature of polyarabinoglucuronoxylan [82], with its multiple hydroxyl (-OH) and carboxyl (-COOH) groups, imparts a hydrophilic character and a strong capacity to form hydrogen bonds, which directly influences its thermal and barrier properties.

Thermal analysis reveals crucial data regarding the processability of CBG: High thermal stability being a significant advantage. This indicates that the polymer can be subjected to elevated temperatures, such as those required for heat sealing, without undergoing chemical degradation. This was confirmed by TGA and DSC calorimetry, which showed no changes between the original film (CBG) and the heat-sealed film (CBG-H), ensuring that the sealing process was a physical phenomenon and not chemical degradation. The T_g marks the point at which the polymer transitions from a rigid, glassy state to a softer, rubbery state. To achieve effective sealing, the process temperature must exceed T_g, allowing the polymer chains to move. The presence of a defined melting point suggests that CBG possesses regions with a certain degree of crystallinity. The heat-sealing process, likely carried out at a temperature close to or above T_m, allows the crystalline regions to melt. Upon cooling, the polymer chains of the two contacting surfaces can interdiffuse and recrystallize together, forming a strong, continuous bond [64]. The processing window, defined between T_g and the degradation temperature (>240 °C), is sufficiently wide to allow precise control of the heat-sealing process [14].

Heat sealing induced notable changes in the nanostructure and microstructure of films. X-ray diffraction analysis showed a decrease in the interlaminar spacing ($d_{-spacing}$) from 4.88 nm in the original film (CBG) to 4.66 nm in the heat-sealed film (CBG-H). This reduction indicates that the heating and cooling cycles of heat sealing promote more compact packing of the polymer chains [64]. This structural rearrangement is likely responsible for the improvement in certain properties, such as the water-vapor barrier. The SEM image of the heat-sealed film (CBG-H) reveals a "quasi-homogeneous" seal but with "small voids and holes" [83]. This observation is significant. While the process successfully bonded the surfaces, the presence of these micrometric defects acted as stress concentration points, explaining the reduction in the mechanical properties of the CBG-H sample. These voids can also compromise the integrity of the material barrier.

The tensile properties and sealing strength were strongly dependent on the process conditions: the original film (CBG) had a Young's modulus of 132 MPa. Interestingly, the heat-sealed film CBG-H was less stiff (96.8 MPa), whereas CBG-V was stiffer (159 MPa). The reduction in the stiffness of CBG-H can be attributed to the defects (voids) observed in the SEM, which disrupt the continuity of the polymer matrix. In contrast, "CBG-V" sealing conditions (possibly different pressure or temperature parameters) not only prevent this weakening but also improve the material stiffness, likely by achieving a more homogeneous seal and better consolidation of the structure [84]. The sealing force values support this hypothesis. The CBG-V seal is considerably stronger (950 N/m) than the CBG-H seal (656 N/m) [61,70]. This directly correlates with the mechanical properties and morphology: a stiffer material and a more homogeneous seal (as inferred for CBG-V) result in a much stronger bond between the two. The lower force in CBG-H is a direct consequence of the structural defects that act as failure points [68].

Heat sealing under optimal conditions dramatically improved the water vapor barrier. The WVP was reduced from 1.7 for the CBG film to 0.37 ng m/m^2 s Pa for the CBG-V film. This substantial improvement is a direct result of the compaction of the polymer

structure (lower $d_{-spacing}$), which creates a more tortuous route for the diffusion of water molecules [85].

The fact that proximate analyses, antioxidant capacity, DSC, and TGA showed no changes between CBG and CBG-H is a valuable finding. This confirms that heat sealing is a purely physical process that does not alter the chemical composition or functional properties (such as antioxidant activity) of the polymer. This is critical for food packaging applications, where preserving the material's quality and preventing the migration of degradation byproducts are imperative [86].

5. Conclusions

Chañar brea gum, due to its high molecular weight, forms films with base properties suitable for packaging applications. CBG films can be effectively heat-sealed without undergoing chemical degradation or losing their antioxidant properties, which is crucial for food applications. The heat-sealing process induces a structural rearrangement that compacts the polymer chains, resulting in a very significant improvement in the water vapor barrier. The performance of heat-sealed materials is highly dependent on the process parameters, especially the seal orientation. The vertical method (CBG-V) was superior in terms of both mechanical and sealing strengths. The presence of morphological defects (voids) in the horizontal seal (CBG-H) suggests that the sealing conditions (temperature and time) can be optimized to achieve a more homogeneous bond.

CBG is emerging as an excellent candidate for developing biodegradable and active bioplastics for food packaging. Its heat sealability, combined with its improved moisture barrier and retention of antioxidant activity, positions it favorably compared to other biopolymers. Future work should focus on optimizing the heat-sealing process to minimize defects and maximize the reproducibility of the excellent properties observed in the vertical configuration.

Author Contributions: Conceptualization, M.F.T. and M.M.; methodology, G.M., F.B. and M.F.T.; validation, M.F.T. and G.M.; formal analysis, M.F.T., M.F. and M.M.; investigation, M.F. and F.B.; resources, M.M.; writing—original draft preparation, M.F.T. and M.M.; writing—review and editing, M.F.T., M.F. and M.M. All authors have read and agreed to the published version of the manuscript.

Funding: PICT-2020-SERIEA-00895 (RAICES). Title: "Obtención de Polisacáridos a partir de Vegetales y Microorganismos de la Región del Semiárido de San Luis. Aplicaciones: Alimentarias, Geles y Bioempaque", 2. PROICO 2-3423, UNSL: "Bioprospección de Recursos Autóctonos Vegetales y Microbianos de la Provincia de San Luis con Potencial Uso Biotecnológico", and 3. PIP 2021/2023, IF-2021-85081432-APN-DCP#CONICET, "Valorización biotecnológica de efluentes de destilería para la obtención de productos microbianos". Institutional Research Program (UNSL): Desarrollo sostenible de productos alimenticios empleando un recurso regional como la goma brea, (2021–2022) (Res. CS 236/21).

Data Availability Statement: The original contributions presented in this study are included in this article. Further inquiries should be directed to the corresponding authors.

Acknowledgments: The authors thank the following institutions in Argentina: Instituto de Física Aplicada (INFAP-UNSL-CONICET) and Laboratorio de Investigación y Servicios de Química Física (LISeQF-UNSL). The authors also thank Javier Rigau from the Instituto de Investigación en Tecnología Química (INTEQUI-UNSL-CONICET) for their determinations of the FTIR, TGA, and DSC, and Ariel Ochoa from the Laboratorio de Membranas y Biomateriales del INFAP-CONICET-UNSL for their contributions to the mechanical test and water vapor permeability results.

Conflicts of Interest: The authors declare no conflicts of interest.

References

1. Das, M.; Chowdhury, T. Heat sealing property of starch based self-supporting edible films. *Food Packag. Shelf Life* **2016**, *9*, 64–68. [CrossRef]
2. Khodaei, D.; Álvarez, C.; Mullen, A.M. Biodegradable packaging materials from animal processing co-products and wastes: An overview. *Polymers* **2021**, *13*, 2561. [CrossRef] [PubMed]
3. Jeevahan, J.J.; Chandrasekaran, M.; Venkatesan, S.P.; Sriram, V.; Joseph, G.B.; Mageshwaran, G.; Durairaj, R.B. Scaling up difficulties and commercial aspects of edible films for food packaging: A review. *Trends Food Sci. Technol.* **2020**, *100*, 210–222. [CrossRef]
4. Dag, D.; Jung, J.; Zhao, Y. Development and characterization of cinnamon essential oil incorporated active, printable and heat sealable cellulose nanofiber reinforced hydroxypropyl methylcellulose films. *Food Packag. Shelf Life* **2023**, *39*, 101153. [CrossRef]
5. Yi, C.; Yuan, T.; Xiao, H.; Ren, H.; Zhai, H. Hydrophobic-modified cellulose nanofibrils (CNFs)/chitosan/zein coating for enhancing multi-barrier properties of heat-sealable food packaging materials. *Colloids Surf. A Physicochem. Eng. Asp.* **2023**, *666*, 131245. [CrossRef]
6. Rajeshkumar, L.; Ramesh, M.; Bhuvaneswari, V.; Balaji, D.; Deepa, C. Synthesis and thermomechanical properties of bioplastics and biocomposites: A systematic review. *J. Mater. Chem. B* **2023**, *11*, 3307–3337. [CrossRef]
7. Kalina, S.; Kapilan, R.; Wickramasinghe, I.; Navaratne, S.B. Potential use of plant leaves and sheath as food packaging materials in tackling plastic pollution: A Review. *Ceylon J. Sci.* **2024**, *53*, 21–37. [CrossRef]
8. Zink, J.; Wyrobnik, T.; Prinz, T.; Schmid, M. Physical, chemical and biochemical modifications of protein-based films and coatings: An extensive review. *Int. J. Mol. Sci.* **2016**, *17*, 1376. [CrossRef]
9. Song, X.; Zuo, G.; Chen, F. Effect of essential oil and surfactant on the physical and antimicrobial properties of corn and wheat starch films. *Int. J. Biol. Macromol.* **2018**, *107*, 1302–1309. [CrossRef]
10. Liu, C.; Huang, J.; Zheng, X.; Liu, S.; Lu, K.; Tang, K.; Liu, J. Heat sealable soluble soybean polysaccharide/gelatin blend edible films for food packaging applications. *Food Packag. Shelf Life* **2020**, *24*, 100485. [CrossRef]
11. Hazarika, K.K.; Konwar, A.; Borah, A.; Saikia, A.; Barman, P.; Hazarika, S. Cellulose nanofiber mediated natural dye based biodegradable bag with freshness indicator for packaging of meat and fish. *Carbohydr. Polym.* **2023**, *300*, 120241. [CrossRef] [PubMed]
12. Alves, Z.; Ferreira, N.M.; Ferreira, P.; Nunes, C. Design of heat sealable starch-chitosan bioplastics reinforced with reduced graphene oxide for active food packaging. *Carbohydr. Polym.* **2022**, *291*, 119517. [CrossRef] [PubMed]
13. Lim, W.S.; Ock, S.Y.; Park, G.D.; Lee, I.W.; Lee, M.H.; Park, H.J. Heat-sealing property of cassava starch film plasticized with glycerol and sorbitol. *Food Packag. Shelf Life* **2020**, *26*, 100556. [CrossRef]
14. Bamps, B.; Buntinx, M.; Peeters, R. Seal materials in flexible plastic food packaging: A review. *Packag. Technol. Sci.* **2023**, *36*, 507–532. [CrossRef]
15. Ren, Z.; Ning, Y.; Xu, J.; Cheng, X.; Wang, L. Eco-friendly fabricating Tara pod extract-soy protein isolate film with antioxidant and heat-sealing properties for packaging beef tallow. *Food Hydrocoll.* **2024**, *153*, 110041. [CrossRef]
16. Trianti, M.; Mastora, A.; Nikolaidou, E.; Zorba, D.; Rozou, A.; Giannou, V.; Tzia, C.; Sinanoglou, V.J.; Papadakis, S.E. Development and characterization of "Greek Salad" edible films. *Food Packag. Shelf Life* **2024**, *46*, 101378. [CrossRef]
17. Wang, R.; Chen, Z.; Shu, Y.; Wang, Y.; Wang, W.; Zhu, H.; Sun, J.; Ma, Q. Apple pectin-based active films to preserve oil: Effects of naturally branched phytoglycogen-curcumin host. *Int. J. Biol. Macromol.* **2024**, *266*, 131218. [CrossRef] [PubMed]
18. Zehra, A.; Amin, T.; Wani, S.M.; Sidiq, H.; Bashir, I.; Mustafa, S.; Showkat, S. Chitosan-Based Films. In *Polysaccharide Based Films for Food Packaging: Fundamentals, Properties and Applications*; Springer Nature: Singapore, 2024; pp. 121–144.
19. Rahman, S.; Konwar, A.; Gurumayam, S.; Borah, J.C.; Chowdhury, D. Sodium Alginate-chitosan-starch based glue formulation for sealing biopolymer films. *Next Mater.* **2025**, *7*, 100507. [CrossRef]
20. Uribarrena, M.; Cabezudo, S.; Núñez, R.N.; Copello, G.J.; de la Caba, K.; Guerrero, P. Development of smart films based on soy protein and cow horn dissolved in a deep eutectic solvent: Physicochemical and environmental assessment. *Int. J. Biol. Macromol.* **2025**, *291*, 139045. [CrossRef]
21. Nafchi, A.M.; Nassiri, R.; Sheibani, S.; Ariffin, F.; Karim, A.A. Preparation and characterization of bionanocomposite films filled with nanorod-rich zinc oxide. *Carbohydr. Polym.* **2013**, *96*, 233–239. [CrossRef]
22. Ortega, F. Materiales Biodegradables Con Nanopartículas de Plata con Capacidad Antimicrobiana Para Mejorar Los Procesos de Conservación de Alimentos. Ph.D. Thesis, Universidad Nacional de la Plata, La Plata, Argentina, 2021.
23. Garavito, J.; Peña-Venegas, C.P.; Castellanos, D.A. Production of Starch-Based Flexible Food Packaging in Developing Countries: Analysis of the Processes, Challenges, and Requirements. *Foods* **2024**, *13*, 4096. [CrossRef] [PubMed]
24. Bertuzzi, M.A.; Slavutsky, A.M.; Armada, M. Physicochemical characterisation of the hydrocolloid from Brea tree (*Cercidium praecox*). *Int. J. Food Sci. Technol.* **2012**, *47*, 768–775. [CrossRef]
25. Bertuzzi, M.A.; Slavutsky, A.M. Formulation and Characterization of Film Based on Gum Exudates from Brea Tree (*Cercidium praecox*). *J. Food Sci. Eng.* **2013**, *3*, 113–122.

26. Slavutsky, A.M.; Bertuzzi, M.A.; Armada, M.; García, M.G.; Ochoa, N.A. Preparation and characterization of montmorillonite/brea gum nanocomposites films. *Food Hydrocoll.* **2014**, *35*, 270–278. [CrossRef]
27. Slavutsky, A.M.; Bertuzzi, M.A. Thermodynamic study of water sorption and water barrier properties of nanocomposite films based on brea gum. *Appl. Clay Sci.* **2015**, *108*, 144–148. [CrossRef]
28. Cecchini, J.P.; Spotti, M.J.; Piagentini, A.M.; Milt, V.G.; Carrara, C.R. Development of edible films obtained from submicron emulsions based on whey protein concentrate, oil/beeswax and brea gum. *Food Sci. Technol. Int.* **2017**, *23*, 371–381. [CrossRef] [PubMed]
29. Slavutsky, A.M.; Gamboni, J.E.; Bertuzzi, M.A. Formulation and characterization of bilayer films based on Brea gum and Pectin. *Braz. J. Food Technol.* **2018**, *21*, e2017213. [CrossRef]
30. Masuelli, M.A.; Slatvustky, A.; Ochoa, A.; Bertuzzi, M.A. Physicochemical Parameters for Brea Gum Exudate from Cercidium praecox Tree. *Colloids Interfaces* **2018**, *2*, 72. [CrossRef]
31. Torres, M.F.; Lazo Delgado, L.; Filippa, M.; Masuelli, M.A. Effect of Temperature on Mark-Houwink-Kuhn-Sakurada (MHKS) Parameters of Chañar Brea Gum Solutions. *J. Polym. Biopolym. Phys. Chem.* **2020**, *8*, 28–30.
32. Torres, M.F.; Lazo Delgado, L.; D'Amelia, R.; Filippa, M.; Masuelli, M. Sol/gel transition temperature of chañar brea gum. *Curr. Trends Polym. Sci.* **2021**, *20*, 83–93.
33. Becerra, F.; Garro, M.F.; Melo, G.; Masuelli, M. Preparation and Characterization of Lithraea molleoides Gum Flour and Its Blend Films. *Processes* **2024**, *12*, 2506. [CrossRef]
34. *ASTM F88-09*; Standard Test Method for Seal Strength of Flexible Barrier Materials. Annual book of ASTM. American Society for Testing and Materials: West Conshohocken, PA, USA, 2009.
35. AOAC International. *Official Methods of Analysis*, 19th ed.; AOAC International: Gaithersburg, MD, USA, 2012.
36. Rulli, M.M.; Villegas, L.B.; Barcia, C.S.; Colin, V.L. Bioconversion of sugarcane vinasse into fungal biomass protein and its potential use in fish farming. *J. Environ. Chem. Eng.* **2021**, *9*, 106136. [CrossRef]
37. Deng, C.; Hu, Z.; Fu, H.; Hu, M.; Xu, X.; Chen, J. Chemical analysis and antioxidant activity in vitro of β-D-glucan isolated from Dictyophora indusiate. *Int. J. Biol. Macromol.* **2012**, *51*, 70–75. [CrossRef]
38. Kaur, R.; Arora, S.; Singh, B. Antioxidant activity of the phenol rich fractions of leaves of Chukrasia tabularis A. Juss. *Bioresour. Technol.* **2008**, *99*, 7692–7698. [CrossRef] [PubMed]
39. Ainsworth, E.A.; Gillespie, K.M. Estimation of total phenolic content and other oxidation substrates in plant tissues using Folin-Ciocalteu reagent. *Nat. Protoc.* **2007**, *2*, 875–877. [CrossRef] [PubMed]
40. Zanon, M.; Masuelli, M. Purification and characterization of alcayota gum. *Biopolym. Res.* **2018**, *2*, 105.
41. Al Sagheer, F.A.; Al-Sughayer, M.A.; Muslim, S.; Elsabee, M.Z. Extraction and characterization of chitin and chitosan from marine sources in Arabian Gulf. *Carbohydr. Polym.* **2009**, *77*, 410–419. [CrossRef]
42. Barbosa, H.F.; Francisco, D.S.; Ferreira, A.P.; Cavalheiro, É.T. A new look towards the thermal decomposition of chitins and chitosans with different degrees of deacetylation by coupled TG-FTIR. *Carbohydr. Polym.* **2019**, *225*, 115232. [CrossRef]
43. Zanon, M.; Masuelli, M.A. Alcayota gum films: Experimental reviews. *J. Mater. Sci. Chem. Eng.* **2018**, *6*, 11–58. [CrossRef]
44. Masuelli, M.A.; Lazo, L.; Becerra, F.; Torres, F.; Illanes, C.O.; Takara, A.; Auad, M.L.; Bercea, M. Physical and Chemical Properties of Pachycymbiola brasiliana Eggshells-From Application to Separative Processes. *Processes* **2024**, *12*, 814. [CrossRef]
45. *ASTM D882-18*; Standard Test Method for Tensile Properties of Thin Plastic Sheeting. American Society for Testing and Materials: West Conshohocken, PA, USA, 2018.
46. Ruano, P.; Delgado, L.L.; Picco, S.; Villegas, L.; Tonelli, F.; Merlo, M.E.A.; Rigau, J.; Masuelli, M. Extraction and Characterization of Pectins from Peels of Criolla Oranges (*Citrus sinensis*): Experimental Reviews. In *Pectins-Extraction, Purification, Characterization and Applications*; Martin, M., Ed.; IntechOpen: London, UK, 2019.
47. *ASTM E96*; Standard Test Methods for Water Vapor Transmission of Materials. American Society for Testing and Materials: West Conshohocken, PA, USA, 2014.
48. Lazo, L.; Melo, G.M.; Auad, M.L.; Filippa, M.; Masuelli, M.A. Synthesis and characterization of Chañar gum films. *Colloids Interfaces* **2022**, *6*, 10. [CrossRef]
49. Illanes, C.O.; Takara, E.A.; Masuelli, M.A.; Ochoa, N.A. pH-responsive gum tragacanth hydrogels for high methylene blue adsorption. *J. Chem. Technol. Biotechnol.* **2024**, *99*, 31–39. [CrossRef]
50. Adhikary, N.D.; Bains, A.; Sridhar, K.; Kaushik, R.; Chawla, P.; Sharma, M. Recent advances in plant-based polysaccharide ternary complexes for biodegradable packaging. *Int. J. Biol. Macromol.* **2023**, *253*, 126725. [CrossRef]
51. Acosta-Ferreira, S.; Castillo, O.S.; Madera-Santana, J.T.; Mendoza-García, D.A.; Núñez-Colín, C.A.; Grijalva-Verdugo, C.; Villa-Lerma, A.G.; Morales-Vargas, A.T.; Rodríguez-Núñez, J.R. Production and physicochemical characterization of chitosan for the harvesting of wild microalgae consortia. *Biotechnol. Rep.* **2020**, *28*, e00554. [CrossRef]
52. Chel-Guerrero, L.; Betancur-Ancona, D.; Aguilar-Vega, M.; Rodríguez-Canto, W. Films properties of QPM corn starch with Delonix regia seed galactomannan as an edible coating material. *Int. J. Biol. Macromol.* **2024**, *255*, 128408. [CrossRef]

53. Yazdi, M.K.; Seidi, F.; Jin, Y.; Zarrintaj, P.; Xiao, H.; Esmaeili, A.; Habibzadeh, S.; Saeb, M.R. Crystallization of polysaccharides. *Polysacch. Prop. Appl.* **2021**, 283–300. [CrossRef]
54. Luo, A.; Hu, B.; Feng, J.; Lv, J.; Xie, S. Preparation, and physicochemical and biological evaluation of chitosan Arthrospira platensis polysaccharide active films for food packaging. *J. Food Sci.* **2021**, *86*, 987–995. [CrossRef]
55. Nahas, E.O.; Furtado, G.F.; Lopes, M.S.; Silva, E.K. From Emulsions to Films: The Role of Polysaccharide Matrices in Essential Oil Retention Within Active Packaging Films. *Foods* **2025**, *14*, 1501. [CrossRef]
56. Du, B.; Jeepipalli, S.P.; Xu, B. Critical review on alterations in physiochemical properties and molecular structure of natural polysaccharides upon ultrasonication. *Ultrason. Sonochemist.* **2022**, *90*, 106170. [CrossRef]
57. Demircan, B.; McClements, D.J.; Velioglu, Y.S. Next-Generation Edible Packaging: Development of Water-Soluble, Oil-Resistant, and Antioxidant-Loaded Pouches for Use in Noodle Sauces. *Foods* **2025**, *14*, 1061. [CrossRef]
58. Bumbudsanpharoke, N.; Harnkarnsujarit, N.; Chongcharoenyanon, B.; Kwon, S.; Ko, S. Enhanced properties of PBAT/TPS biopolymer blend with CuO nanoparticles for promising active packaging. *Food Packag. Shelf Life* **2023**, *37*, 101072. [CrossRef]
59. Dong, Y.; Rao, Z.; Liu, Y.; Zheng, X.; Tang, K.; Liu, J. Soluble soybean polysaccharide/gelatin active edible films incorporated with curcumin for oil packaging. *Food Packag. Shelf Life* **2023**, *35*, 101039. [CrossRef]
60. Bhat, R.; Abdullah, N.; Din, R.H.; Tay, G.S. Producing novel sago starch based food packaging films by incorporating lignin isolated from oil palm black liquor waste. *J. Food Eng.* **2013**, *119*, 707–713. [CrossRef]
61. Sadegh-Hassani, F.; Nafchi, A.M. Preparation and characterization of bionanocomposite films based on potato starch/halloysite nanoclay. *Int. J. Biol. Macromol.* **2014**, *67*, 458–462. [CrossRef]
62. Chhikara, S.; Kumar, D. Edible coating and edible film as food packaging material: A review. *J. Packag. Technol. Res.* **2022**, *6*, 1–10. [CrossRef]
63. Kim, S.J.; Ustunol, Z. Thermal properties, heat sealability and seal attributes of whey protein isolate/lipid emulsion edible films. *J. Food Sci.* **2001**, *66*, 985–990. [CrossRef]
64. Nafchi, A.M. Mechanical, barrier, physicochemical, and heat seal properties of starch films filled with nanoparticles. *J. Nano Res.* **2013**, *25*, 90–100. [CrossRef]
65. Shah, Y.A.; Bhatia, S.; Al-Harrasi, A.; Oz, F.; Khan, M.H.; Roy, S.; Esatbeyoglu, T.; Pratap-Singh, A. Thermal properties of biopolymer films: Insights for sustainable food packaging applications. *Food Eng. Rev.* **2024**, *16*, 497–512. [CrossRef]
66. Demircan, B.; Velioglu, Y.S. Revolutionizing single-use food packaging: A comprehensive review of heat-sealable, water-soluble, and edible pouches, sachets, bags, or packets. *Crit. Rev. Food Sci. Nutr.* **2025**, *65*, 1497–1517. [CrossRef]
67. Chu, Y. *Regenerated Cellulose Films with Heat Sealability and Improved Barrier Properties for Sustainable Food Packaging*; McGill University: Montreal, QC, Canada, 2023.
68. Cho, S.W.; Ullsten, H.; Gällstedt, M.; Hedenqvist, M.S. Heat-sealing properties of compression-molded wheat gluten films. *J. Biobased Mater. Bioenergy* **2007**, *1*, 56–63. [CrossRef]
69. Rouhi, J.; Mahmud, S.; Naderi, N.; Ooi, C.R.; Mahmood, M.R. Physical properties of fish gelatin-based bio-nanocomposite films incorporated with ZnO nanorods. *Nanoscale Res. Lett.* **2013**, *8*, 364. [CrossRef]
70. Roidoung, S.; Sonyiam, S.; Fugthong, S. Development of heat sealable film from tapioca and potato starch for application in edible packaging. *J. Food Sci. Technol.* **2025**, *62*, 389–395. [CrossRef] [PubMed]
71. Aleksanyan, K.V. Polysaccharides for biodegradable packaging materials: Past, present, and future (Brief Review). *Polymers* **2023**, *15*, 451. [CrossRef]
72. Zhao, Y.; Li, B.; Li, C.; Xu, Y.; Luo, Y.; Liang, D.; Huang, C. Comprehensive review of polysaccharide-based materials in edible packaging: A sustainable approach. *Foods* **2021**, *10*, 1845. [CrossRef] [PubMed]
73. Zhao, F.; Jiang, L.; Wang, C.; Li, S.; Sun, D.; Ma, Q.; Yu, Z.; Liu, Y.; Jiang, W. Flexibility, dissolvability, heat-sealability, and applicability improvement of pullulan-based composite edible films by blending with soluble soybean polysaccharide. *Ind. Crops Prod.* **2024**, *215*, 118693. [CrossRef]
74. López, O.V.; Lecot, C.J.; Zaritzky, N.E.; García, M.A. Biodegradable packages development from starch based heat sealable films. *J. Food Eng.* **2011**, *105*, 254–263. [CrossRef]
75. Chu, Y.; Popovich, C.; Wang, Y. Heat sealable regenerated cellulose films enabled by zein coating for sustainable food packaging. *Compos. Part C Open Access* **2023**, *12*, 100390. [CrossRef]
76. Jongjun, Y.; Pornprasert, P.; Prateepchanachai, S. Improvement of heat-sealing strength of chitosan-based composite films and product costs analysis in the production process. *J. Appl. Res. Sci. Technol.* **2024**, *23*, 251817. [CrossRef]
77. Zhang, H.; Li, M.; Liu, Z.; Li, R.A.; Cao, Y. Heat-sealable, transparent, and degradable arabinogalactan/polyvinyl alcohol films with UV-shielding, antibacterial, and antioxidant properties. *Int. J. Biol. Macromol.* **2024**, *275*, 133535. [CrossRef]
78. Fernandes, S.S.; Romani, V.P.; da Silva Filipini, G.; G Martins, V. Chia seeds to develop new biodegradable polymers for food packaging: Properties and biodegradability. *Polym. Eng. Sci.* **2020**, *60*, 2214–2223. [CrossRef]
79. Janik, W.; Nowotarski, M.; Shyntum, D.Y.; Bana, A.; Krukiewicz, K.; Kudła, S.; Dudek, G. Antibacterial and biodegradable polysaccharide-based films for food packaging applications: Comparative study. *Materials* **2022**, *15*, 3236. [CrossRef] [PubMed]

80. Masuelli, M.A.; García, M.G. Biopackaging: Tara Gum Films. In *Advances in Physicochemical Properties of Biopolymers*; Part 2; Martin, M., Denis, R., Eds.; Bentham Publishing: Dubai, United Arab Emirates, 2017; pp. 876–898.
81. García, M.G.; Masuelli, M.A. Effect of Cross-Linking Agent on Mechanical and Permeation Properties of Criolla Orange Pectin. In *Pectin-The New-Old Polysaccharides*; Martin, M., Ed.; INTECH: Rijeka, Croatia, 2022.
82. Sznaider, F.; Stortz, C.A.; Rojas, A.M.; Navarro, D.A. Cercidium praecox brea gum arabinoglucuronoxylans: A viscosant substitute for gum Arabic? *Food Hydrocoll.* **2023**, *137*, 108403. [CrossRef]
83. Ferreira, A.R.; Torres, C.A.; Freitas, F.; Reis, M.A.; Alves, V.D.; Coelhoso, I.M. Biodegradable films produced from the bacterial polysaccharide FucoPol. *Int. J. Biol. Macromol.* **2014**, *71*, 111–116. [CrossRef]
84. Mukherjee, C.; Varghese, D.; Krishna, J.S.; Boominathan, T.; Rakeshkumar, R.; Dineshkumar, S.; Rao, B.; Sivaramakrishna, A. Recent advances in biodegradable polymers–properties, applications and future prospects. *Eur. Polym. J.* **2023**, *192*, 112068. [CrossRef]
85. Long, J.; Zhang, W.; Zhao, M.; Ruan, C.Q. The reduce of water vapor permeability of polysaccharide-based films in food packaging: A comprehensive review. *Carbohydr. Polym.* **2023**, *321*, 121267. [CrossRef]
86. Versino, F.; Ortega, F.; Monroy, Y.; Rivero, S.; López, O.V.; García, M.A. Sustainable and bio-based food packaging: A review on past and current design innovations. *Foods* **2023**, *12*, 1057. [CrossRef]

Disclaimer/Publisher's Note: The statements, opinions and data contained in all publications are solely those of the individual author(s) and contributor(s) and not of MDPI and/or the editor(s). MDPI and/or the editor(s) disclaim responsibility for any injury to people or property resulting from any ideas, methods, instructions or products referred to in the content.